

INVESTIGATIONS ON THE EFFECT OF THE NOZZLE MATERIAL ON THE INTERRUPTION CAPABILITY OF A MEDIUM VOLTAGE LOAD BREAK SWITCH

M.BENDIG^{a,*}, T. KRAMPERT^a, N. GÖTTE^a, A. KALTER^b, M. SCHAAK^b,
K. ERMELER^c

^a Institute for High Voltage Technology, RWTH Aachen University, Schnikelstr. 2, 52056 Aachen, Germany

^b Siemens AG, Energy Management Division, Carl-Benz-Str. 22, 60386 Frankfurt am Main, Germany

^c Siemens AG, Energy Management Division, Nonnendammallee 104, 13629 Berlin, Germany

* bendig@ifht.rwth-aachen.de

Abstract. In the process of substituting sulphur hexafluoride in medium voltage load break switches by atmospheric gases, the inferior arc quenching capabilities of possible substitutes have to be compensated. By introducing a polymer nozzle into the switching gap of a load break switch, the interruption capability can be enhanced as the ablated nozzle material changes the composition of the arc plasma. In this contribution the interruption capability of a model load break switch is investigated using different nozzle materials. The results show a good interruption capability when using polypropylene and polyamide 6.6 for high blowing pressures. Polytetrafluorethylene shows good results across a wide blowing pressure range. Polylactide has the lowest interruption capability among the polymers in this work.

Keywords: load break switch, nozzle material, ablation, alternative gases.

1. Introduction

Medium voltage load break switches (LBS) are widely used switchgear in the secondary distribution grid. They serve as combined load and disconnecter switches and are capable of interrupting load currents in the range of a few hundred amps. Due to the space limitations in urban areas LBS are mainly built into metal-enclosed switchgear filled with the insulation gas sulphur hexafluoride (SF_6). SF_6 , with its high dielectric strength and superior arc quenching capabilities, allows for a compact and reliable switchgear design. Nevertheless, SF_6 has a global warming potential of 23500 carbon dioxide (CO_2) mass equivalents, which makes it the most potent greenhouse gas known. Possible atmospheric substitutes like air or CO_2 have been investigated in previous works. As their arc quenching capability is inferior to SF_6 , additional measures like an axial arc blowing have to be applied [1, 2]. One way of enhancing the interruption capability of a gas switch is by introducing a gassing polymer nozzle into the switching gap. If a switching arc is drawn between the contacts, the polymer ablates and the released gas is changing the composition of the plasma. It has been shown, that polymers that release either fluorine or hydrogen are good candidates to be used as a nozzle in LBS [3, 4].

This work analyses the influence of the applied nozzle material on the interruption capability of a model load break switch. The investigated polymers are polytetrafluorethylene (PTFE), as a polymer releasing fluorine as well as polypropylene (PP), polyamide 6.6

(PA6.6) and polylactide (PLA) as polymers releasing hydrogen. All tests were performed using a nitrogen - carbon dioxide mixture as quenching and insulation gas at an elevated filling pressure of $p = 1800$ hPa absolute to enhance the electric strength.

2. Experimental method

To evaluate the switching performance the thermal interruption capability as well as the rate of the dielectric recovery are determined individually. By using this method, the effects of the used nozzle material can be analyzed for the different phases.

2.1. Thermal interruption limit

A successful thermal interruption is dependent on the current steepness shortly before current zero (CZ) as well as on the voltage steepness shortly after CZ. In this work the critical current steepness di/dt_{crit} is used to quantify the thermal interruption capability. For the determination the synthetic test circuit shown in Figure 1 is used. The high current circuit provides one half oscillation of a sinusoidal current with a value of $I_{\text{rms}} = 630$ A and a frequency of $f_1 \approx 50$ Hz. Shortly before the current reaches its natural CZ the thyristor in the high voltage circuit is triggered and a current with an amplitude in the range of a few ten amps and a frequency of $f_2 \approx 1000$ Hz is superimposed over the test current. Using this superposition method, the current steepness at CZ can be varied independent of the test current amplitude. When the current is interrupted successfully a recovery voltage rises across the

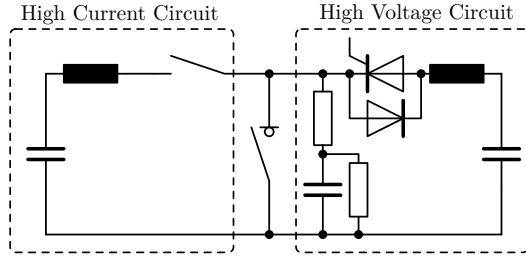


Figure 1. Test circuit to determine the thermal interruption capability

open contacts. To set the rate of rise of the recovery voltage (RRRV) a parallel resistor with $R_p = 220 \Omega$ is used. This resistor is chosen in a way that the RRRV corresponds to the RRRV of a standardized test for $U_N = 24 \text{ kV}$ when a current steepness according to the steepness of a 630 A test at a frequency of $f = 50 \text{ Hz}$ is set. As the parallel resistor is fixed, the RRRV changes when the current steepness is changed.

At the beginning of a test series a low current steepness (di/dt) is chosen and five successful interruption tests are performed. Afterwards the di/dt is increased and another five interruptions are performed. This procedure is repeated until all five interruptions for one di/dt fail. Afterwards the measured di/dts and RRRVs are plotted into a diagram and a linear regression is performed to make sure that all tests have the right ratio between di/dt and RRRV. In a next step the critical RRRV is determined as the mean value between the lowest failed test and the next lowest successful test. Afterwards, the critical current steepness is determined as the product of the regression slope and the critical RRRV. By using this method, inaccuracies from the low signal to noise ratio of the current signal around CZ are avoided.

2.2. Dielectric recovery

The dielectric recovery of the model switch is determined with the test method and circuit described in [5]. The test object is stressed with a half oscillation of a current with a value of $I_{\text{rms}} = 630 \text{ A}$. Afterwards, the breakdown voltage at a certain delay after CZ is determined by applying a steep impulse voltage to the test object. This procedure is repeated for several delay times to get a time resolved course of the breakdown voltage after current zero. For each delay time a minimum of four breakdown tests is performed.

3. Test setup

A sectional view of the model switch is shown in Figure 2. The contact system consists of a combination of a tulip and a pin contact made from a tungsten-copper alloy with a weight ratio of 80/20. The maximum contact distance is $s = 58,5 \text{ mm}$ and the contact diameter of the pin is $d_c = 10 \text{ mm}$. The switching arc is cooled by an axial blowing through the tulip contact. The blowing is initiated by a magnetic valve, which is connected to an external gas volume. The blowing

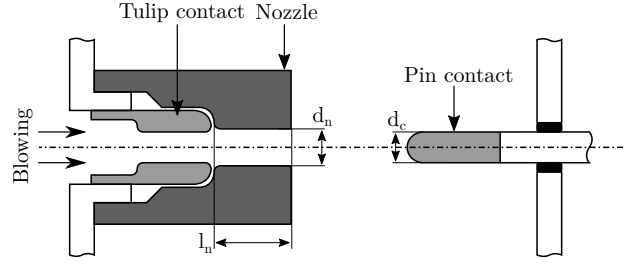


Figure 2. Section of the model load break switch

Property	PTFE	PP	PA6.6	PLA
ρ [g/cm ³]	2.16	0.91	1.15	1.15
T_L [°C]	≈ 330	≈ 160	260	215
Color	Gray	Gray	Natural	White
Vapor	F	H	H	-

Table 1. Properties of the investigated polymers

pressure is measured upstream of the nozzle using a Pitot probe and is given as the total pressure drop across the tulip and nozzle. All investigated pressures in this work lead to a subsonic flow. The tulip contact and part of the contact distance is surrounded by a polymer nozzle with a nozzle throat diameter of $d_n = 11 \text{ mm}$ and a nozzle throat length of $l_n = 24 \text{ mm}$. This configuration was identified as a good parameter set in previous work [1]. The investigated nozzle materials in this work are shown in Table 1. The density ρ as well as the melting point T_L vary across the different materials. While the used PTFE, PP and PLA are colored, the PA6.6 is used in its natural ivory color. If ablated by the arc, the resulting vapor mainly consists of fluorine for PTFE and hydrogen for PP and PA6.6 [4, 6, 7]. For PLA no data was found on the ablation behavior. All nozzles are milled except of the PLA nozzle, which is 3D printed. Due to the manufacturing the internal surface as well as the structure of the material differs from the other nozzles.

The model switch is operated by a pneumatic piston drive with a stroke of 90 mm and an average opening speed of $v_m = 4,5 \text{ m s}^{-1}$. The stroke is recorded during the opening process using a laser triangulation measurement system.

4. Results

The thermal interruption capability is tested for nozzles made from PTFE, PP, PA6.6 and PLA. The dielectric recovery is only analyzed for PTFE, PP and PA 6.6. Additionally the mass losses due to ablation are determined for all investigated materials.

4.1. Thermal interruption capability

The critical current steepnesses for the different materials are shown in Figure 3 for different blowing pressures. The lines are drawn for better visualization. For the maximum blowing pressure and when using PP or

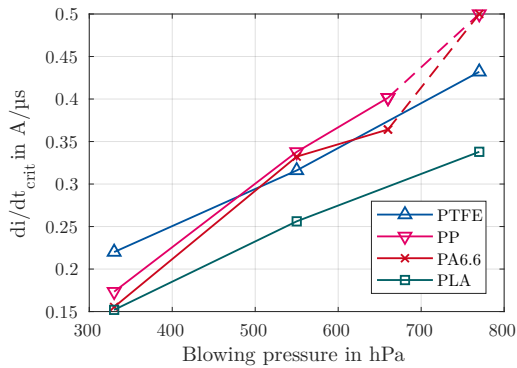


Figure 3. Thermal interruption capability for different nozzle materials and blowing pressures

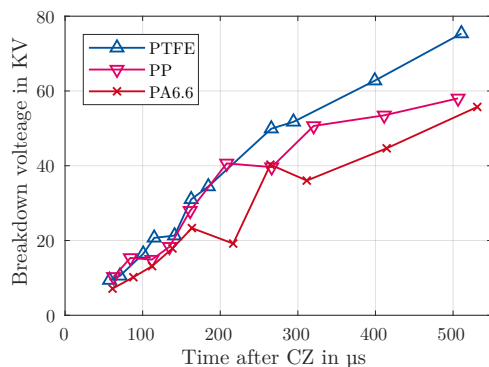


Figure 4. Dielectric recovery after current zero for different nozzle materials

PA6.6 no thermal failure occurs with the maximum steepness of the test circuit $di/dt_{\max} = 0,5 \text{ A } \mu\text{s}^{-1}$. Dashed lines indicate that the critical steepness is above this level.

For all investigated nozzle materials the critical current steepness rises with increasing blowing pressure. However, there are differences in the pressure dependence. When using PTFE or PLA as a nozzle material, the increase in interruption capability rises nearly parallel for a rising blowing pressure, with PTFE showing significantly higher critical current steepnesses. When using either PP or PA6.6 the critical current steepnesses are low for low blowing pressures but the increase with pressure is much higher than for PTFE or PLA.

4.2. Dielectric recovery

The time resolved breakdown voltages after CZ are shown in Figure 4 for PTFE, PP and PA6.6. PLA was not investigated due to its low thermal interruption capability. The plotted values represent the mean values of at least four breakdowns at one specific delay time. The blowing pressure is set to $p = 330 \text{ hPa}$ for all tests.

For all investigated nozzles a strong increase in breakdown voltage occurs after current zero. In the first $170 \mu\text{s}$ the difference between the nozzle materials is low. Afterwards PA6.6 shows a slight decrease in

Material	PTFE	PP	PA6.6	PLA
Ablation [mg]	3	5.8	5.2	11.5

Table 2. Ablated mass per 630 A half oscillation for the investigated nozzle materials

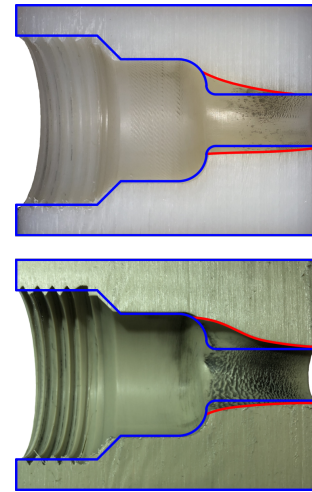


Figure 5. Photos of the PA 6.6 (top) and the PP (bottom) nozzle after 250 switching operations

dielectric strength followed by a slight decrease of the breakdown voltage of PP. Local minima are expected to result from statistical scatter. From roughly $300 \mu\text{s}$ on, the highest breakdown voltages are achieved when using a PTFE nozzle followed by PP and PA6.6.

4.3. Nozzle ablation

To compare the ablation behavior of the different nozzle materials the nozzles are weighed after production and after 100 consecutive interruption tests. Then the average weight loss per 630 A half oscillation is calculated. In Table 2 the resulting ablation masses are given. The ablation rates show large deviations among the different materials. Due to its high sublimation temperature PTFE shows the lowest weight loss. The weight losses of PP and PA6.6 are in the same range, despite of their different melting temperatures. However, as the density of PP is lower than of PA6.6 the volumetric losses are higher. PLA shows by far the highest mass losses. This might be due to the 3D printed structure being not as dense as the other nozzles. Furthermore, the significantly higher roughness inside the nozzle throat might lead to increased ablation during switching.

On all nozzles except from the PTFE nozzle a soot formation can be observed after the tests. Photos of the PP and the PA 6.6 nozzle after 250 switching operations are shown in Figure 5. The original geometry is highlighted with a blue curve, while the actual geometry is highlighted by a red curve. The stronger volumetric loss of the PP nozzle is clearly visible. As the arc has a preferred footpoint on the top of the tulip, the maximum ablation occurs there.

5. Discussion

As the different nozzle materials show different effects in the thermal and the dielectric phase the two phases are discussed individually.

5.1. Thermal phase

The ablated vapor of PP and PA6.6 mainly consists of hydrogen. Due to its high thermal conductivity an efficient arc cooling can be achieved. However, the ablated masses are almost twice as high as for PTFE, which leads to a higher pressure rise inside the nozzle due to ablation. It is assumed, that this higher pressure rise leads to a nozzle clogging at lower blowing pressure, resulting in an insufficient flow field and therefore a reduced interruption capability. At higher blowing pressures the pressure rise due to ablation is lower than the external pressure leading to a sufficient flow. The high hydrogen content results in an increased interruption capability in comparison to PTFE.

Due to the lower ablated mass when using PTFE, the effective flow field is more efficient which results in a good interruption capability. As the ablated gas is very similar to dissociated SF₆, an admixture of ablated PTFE to the plasma increases the interruption capability as well [7]. As PLA has a significantly higher ablation rate, the flow is insufficient even at high external blowing pressures.

5.2. Dielectric phase

As the experiments for determining the dielectric recovery are performed with a blowing pressure of $p_b = 330$ hPa, similar effects can be assumed to those in the thermal phase. This leads to PP and PA6.6 having an insufficient cooling and therefore also a slower recovery than PTFE. Additionally, the ablated gas almost completely dissociates in vicinity of the arc. Due to the absence of the highly reactive fluorine conductive carbon black might be formed in the recombination process leading to a lower breakdown voltage and therefore a slower dielectric recovery.

To isolate the effect of carbon black formation, experiments with a higher blowing pressure should be conducted. However, as the recovery voltage at medium voltage load interruption is not as demanding as i.e. during fault interruption, the dielectric recovery in the latter part is sufficient for all investigated cases. Only the first 120 μ s might be critical.

6. Conclusions

The thermal interruption capability as well as the rate of the dielectric recovery were experimentally determined for a model load break switch with an axial arc blowing using different nozzle materials. The following results were obtained:

- PTFE shows a good thermal interruption capability for all investigated blowing pressures as well as a good dielectric recovery, due to its low ablation rate.

- Polymers that release hydrogen in high parts during arcing, like PP and PA6.6, show an increased thermal interruption capability for high blowing pressures. However, due to their higher ablation rate, insufficient cooling may result from clogging at lower blowing pressures.
- The dielectric recovery may be slower when using PP or PA6.6 due to clogging and the formation of carbon black during the recombination process.
- 3D printed PLA is not a suitable nozzle material, as the high ablation rate leads to a low interruption capability.

Summarizing, PTFE is a good candidate for a nozzle material in load break switches using alternative insulation gases. If sufficient blowing pressures are available using PP or PA6.6 can result in an even higher thermal interruption capability. The disadvantage is the higher nozzle wear as well as the formation of soot after switching.

Acknowledgements

This work was supported by the Federal Ministry for Economic Affairs and Energy on the basis of a decision by the German Bundestag.

The authors would like to thank Tim Ballweber for his assistance in this work.

References

- [1] M. Bendig, N. Götte, T. Krampert, A. Schnettler, A. Kalter, and M. Schaak. Investigations on the switching capability of medium voltage load break switches in an alternative quenching gas. In *Proc. of the 22nd Int. Conf. on Gas Discharges and their Applications*, 2018.
- [2] N. Sasaki Aanensen, E. Jonsson, and M. Runde. Air-flow investigation for a medium-voltage load break switch. *IEEE Trans. Power Delivery*, 30(1):299–306, 2015. doi:10.1109/TPWRD.2014.2334360.
- [3] D. Gonzales, H. Pursch, and F. Berger. Experimental investigation of the interaction of interrupting arcs and gassing polymer walls. In *57th Holm Conference on Electrical Contacts*, 2011. doi:10.1109/HOLM.2011.6034774.
- [4] H. Taxt, K. Niayesh, and M. Runde. Medium voltage load current interruption in presence of ablating polymer material. *IEEE Trans. Power Delivery*, 33(5):2535–2540, 2018. doi:10.1109/TPWRD.2018.2803165.
- [5] M. Bendig, N. Götte, T. Krampert, A. Schnettler, A. Kalter, and M. Schaak. A method to determine the rate of the dielectric recovery in a medium voltage load break switch with a free burning switching arc. In *Proc. of the 22nd Int. Conf. on Gas Discharges and their Applications*, 2018.
- [6] P. Andre. Composition and thermodynamic properties of ablated vapours of PMMA, PA6-6, PETP, POM and PE. *J. Phys. D: Appl. Phys.*, 29(7):1963–1972, 1996. doi:10.1088/0022-3727/29/7/033.
- [7] M. Kriegel. *Einfluss des Düsenmaterials auf das Ausschaltverhalten von SF₆-Selbstblassaltern*. Dissertation, RWTH Aachen University, 1999.